Dynamic Modeling of In-Event Interdependencies in Community Resilience

Omar A. Sediek, S.M.ASCE[1]; Sherif El-Tawil, F.ASCE[2]; and Jason McCormick, M.ASCE[3]

Abstract: A simulation-based model designed to conduct in-event simulation for the assessment and quantification of seismic resilience of communities is presented. The proposed simulation approach employs a dynamic analysis that models the behavior of the community at each time step as the seismic event occurs (time step in seconds) and as the community recovers after the event (time step in days). The dynamic nature of the analysis permits explicit consideration of in-event interdependencies that can arise between the physical (i.e., buildings-related) and social (i.e., injured people-related) systems of the community and provides detailed information about the temporal and spatial distribution of injuries/fatalities during the seismic hazard. The proposed model is modularized into independent simulators that model different aspects of the studied scenario, including the city layout, seismic hazard, community losses, and physical and social recovery trajectories. The capability of the proposed simulation model to support hazard mitigation planning was demonstrated through a case study that showed the trade-off between physical and social costs of various feasible mitigation strategies. **DOI: 10.1061/(ASCE)NH.1527-6996.0000413.**

Introduction

Early models for assessment of earthquake impact on a community computed loss as a function of high-level parameters. For example, Chen et al. (1997) proposed an earthquake loss estimation method based on population distribution and gross domestic product. As it became clear that economic and social losses were highly dependent on the physical damage caused by an extreme event, the state-of-the-art evolved toward more-realistic and more-detailed loss models that explicitly accounted for structural response.

A prominent example of damage-based loss estimation methods is the HAZUS methodology (FEMA 2003). HAZUS computes direct and indirect social and economic losses based on building fragility functions. However, it treats a building as a single-degree-of-freedom (SDOF) system, which limits the granularity of the methodology. In particular, losses are assessed at the entire building level and not at the story level. This limitation was solved by the FEMA P-58 (FEMA 2012b) methodology by quantifying the performance of each structural and nonstructural component in the building separately (i.e., different fragilities) in terms of repair time, repair cost, and casualties.

A number of researchers have developed computational frameworks using available damage and loss estimation models to assess earthquake loss and, more broadly, community resilience (Burton et al. 2016, 2017; Vona et al. 2018; Sutley et al. 2017; Cimellaro et al. 2016; Kammouh et al. 2018). Miles and Chang (2003, 2006) proposed a conceptual framework for community recovery, which was extended into a numerical model implemented in ResilUS (Miles and Chang 2011). Cimellaro et al. (2010) simplified the recovery process by defining three types of recovery functions (linear, exponential, and trigonometric) depending on community preparedness. Special attention was given to the recovery and resilience of the healthcare system in a community by Kirsch et al. (2010), Mitrani-Reiser et al. (2012), and Jacques et al. (2014). Hassan and Mahmoud (2018) developed a framework for the assessment of postearthquake functionality of the hospital system in a community based on a set of structural and nonstructural parameters. The framework was extended by Hassan and Mahmoud (2019) to address hospital functionality restoration. Other notable frameworks for community resilience are those of Lin and Wang (2017, 2019) and Masoomi et al. (2018).

Most available frameworks for assessing resilience have key limitations. Many are based on generic loss estimation models (e.g., HAZUS) in which each building is simplified to a fragility curve. Even when finer granularity is taken into account to permit computation of repair time at the component level (e.g., based on FEMA P-58), there frequently is insufficient information about the required number of workers, repair sequences, and delay times needed for accurate and realistic recovery computations. Most of the available recovery models do not accurately consider the availability of resources and the interdependencies between the different infrastructure systems of society during the recovery stage. In addition, the majority of existing frameworks are fully integrated platforms, which makes it difficult to extend them, add new features, or expand their capabilities to address new situations.

Two frameworks were proposed to address the aforementioned shortcomings: IN-CORE, which is being developed by the Center of Excellence for Risk-Based Community Resilience Planning (Ellingwood et al. 2016), and the platform developed by Lin et al. (2019) and applied by Abdelhady et al. (2019). The former is a modular platform, and the latter also is modular and is based on a publish–subscribe data management model implemented within a distributed computing simulation environment. Distributed computing enables executing different models (simulators) across multiple processors (or computers) connected through a communication

[1]Ph.D. Candidate, Dept. of Civil and Environmental Engineering, Univ. of Michigan, Ann Arbor, MI 48109-2125 (corresponding author). ORCID: https://orcid.org/0000-0002-3369-2598. Email: osediek@umich.edu

[2]Professor, Dept. of Civil and Environmental Engineering, Univ. of Michigan, Ann Arbor, MI 48109-2125. ORCID: https://orcid.org/0000-0001-6437-5176. Email: eltawil@umich.edu

[3]Associate Professor, Dept. of Civil and Environmental Engineering, Univ. of Michigan, Ann Arbor, MI 48109-2125. ORCID: https://orcid.org/0000-0002-7379-4660. Email: jpmccorm@umich.edu

Note. This manuscript was submitted on November 6, 2019; approved on June 11, 2020; published online on August 31, 2020. Discussion period open until January 31, 2021; separate discussions must be submitted for individual papers. This paper is part of the ***Natural Hazards Review***, © ASCE, ISSN 1527-6988.

network. The simulation model proposed herein has architectural similarities to these two platforms.

Unlike most previous approaches, the proposed model employs a simulation-based dynamic analysis that models the behavior of the community at each time step as the seismic event occurs (time step in seconds) and as the community recovers after the event (time step in days). Therefore, it permits explicit consideration of in-event interdependencies (i.e., during the hazard as well as the recovery stage) that can arise between the physical (i.e., buildings-related) and social (i.e., injured people–related) systems of the community and provides detailed information about the temporal and spatial distribution of injuries and fatalities during the seismic hazard. This sort of data allows emergency teams to better optimize the utilization of their resources, which results in more-realistic modeling of recovery trajectories.

Another key innovation in this work is the combination of the FEMA P-58 (FEMA 2012b) methodology for loss estimation, which provides detailed information about the spatial distribution of the seismic losses at the component level, and the REDi model (Almufti and Willford 2013) for assessment of downtime, repair schedule, and required number of workers to repair the damaged buildings at the community level. This combination permits evaluation of the recovery path of the community based on realistic repair schedules as well as the availability of workers in the community.

This paper describes the new simulation model and showcases how it can be used to explicitly model in-event interdependencies that arise between the physical (i.e., buildings-related) and social (i.e., injured people–related) systems of the community. The capability of the proposed model to support hazard mitigation planning was demonstrated through a case study that highlighted the trade-off between the physical and social costs of different mitigation strategies.

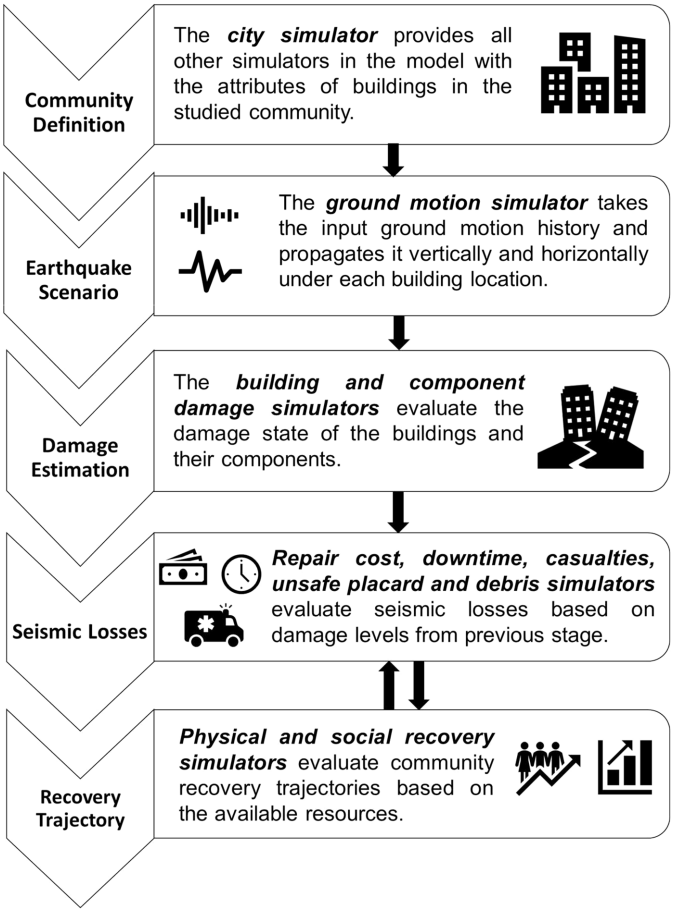

Fig. 1. Proposed simulation model overview.

Simulation Model Overview

The proposed simulation model (Figs. 1 and 2) connects different simulators that model different aspects of the studied scenario, including the city layout, seismic hazard, community losses, and physical and social recovery path simulation. Each simulator can be replaced with another of higher or lower fidelity as long as it takes input and provides output in the same format as the original simulator. For example, the structural analysis simulator computes the structural responses of the buildings (i.e., output) using the ground motion parameters from the ground motion simulator (i.e., input) regardless of the fidelity of the structural model implemented in the structural analysis simulator. It can be as simple as a two-dimensional (2D) elastic representation of the building or as detailed as a three-dimensional (3D) inelastic model.

There are two types of connectivity between the simulators: sequential and interdependent connectivity. In sequential connectivity, the simulators are connected in such a way that the data flow in one direction during each time step. In the latter, the data flow in two directions between the simulators, meaning that both simulators update each other within a time step to account for mutual interdependencies. There are four types of simulators, based on how they are connected to the model (Fig. 2): (1) a simulator that runs once at the beginning of the hazard event and broadcasts initial required data (i.e., city simulator), (2) simulators that run at every time step during the earthquake (time step in seconds), (3) simulators that run once at the end of the hazard event to estimate the initial conditions for the recovery stage (e.g., economic and social losses), and (4) simulators that run at each time step during the recovery stage (time step in days).

Methodology

Problem Setup and Naming Scheme

The city simulator broadcasts information about the community including coordinates, elevation, occupancy, material, structural system, structural and nonstructural component specifications, and quantities of all the buildings to all other simulators. It reads this information from a MATLAB database, providing flexibility in studying any existing, new, or virtual community if the attributes are modeled properly in the MATLAB database. To facilitate the interpretation of building attributes in the studied community, the buildings are designated ABC-D-E (the naming scheme used by Sediek et al. 2019), in which A denotes the material, B denotes the structural system, C denotes the design code, D denotes the number of stories, and E denotes the occupancy of the building. For example, SFC-2-1 is a steel moment frame, old code (pre-1973) 2-story commercial building. The naming scheme used by the city simulator is listed in Table 1.

Demand and Capacity Computations

The ground motion simulator takes the ground motion history at the underlying rock or rocklike layer of a recording station as input. It then performs site response analysis by propagating the ground motion in both directions (i.e., vertically and horizontally) at each time step during the earthquake. To propagate the ground motion vertically through different soil layers, the lumped mass-spring analysis formulated by Idriss and Seed (1968) is used by assuming linearly

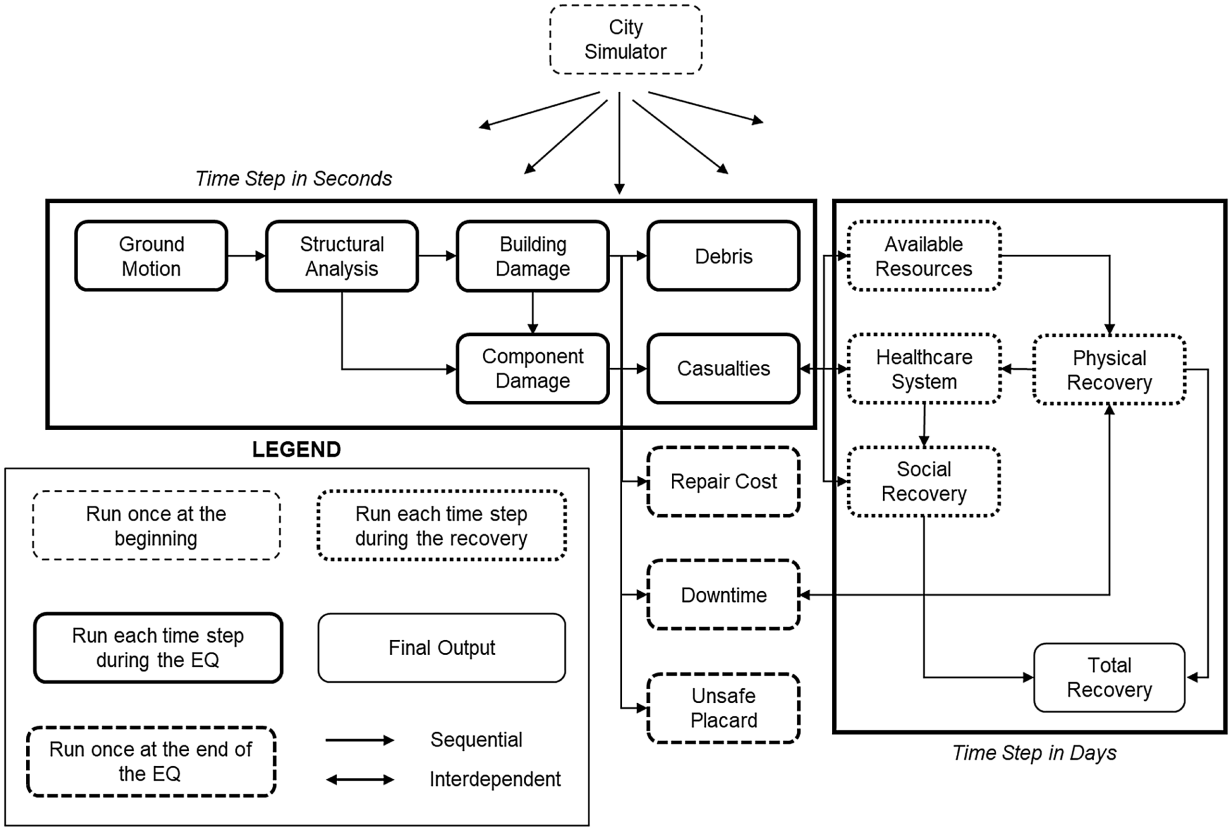

Fig. 2. Schematic diagram of the proposed simulation model.

Table 1. Naming scheme of buildings used by city simulator

Material		Structural system		Design code		Occupancy	
Label	Description	Label	Description	Label	Year	Label	Description
S	Steel	B	Braced frame	A	>1994	1	Commercial
C	Concrete					2	Elementary schools
						3	Middle schools
WS	Small wood (area $< 465\,m^2$)	F	Moment frame	B	1973–1994	4	High schools
						5	Healthcare
WL	Large wood (area $> 465\,m^2$)					6	Hospitality
RM	Reinforced masonry	S	Shear wall	C	<1973	7	Residential buildings
						8	Research laboratories
URM	Unreinforced masonry					9	Retail
						10	Warehouse

elastic soil layers. Then, a Newmark-beta scheme is used to solve the formulated equations of motion. The ground motion history is scaled using the attenuation relationship proposed by Campbell and Bozorgnia (2008) to propagate the ground motion horizontally under each building in the community.

The structural analysis simulator evaluates the dynamic response of each building in the community using nonlinear dynamic analysis in OpenSees (McKenna et al. 2000) based on the ground motion history provided by the ground motion simulator. The structural responses evaluated by the structural analysis simulator then are used to evaluate the damage state (DS) of each building in the community at each time step during the earthquake based on the damage state limits obtained from HAZUS-MH version 2.1 (FEMA 2003). These limit states are based on building attributes such as total height, building area, lateral force resisting system, and the design year.

HAZUS categorizes the building damage into four limit states: slight, moderate, extensive, and complete. More details about the description of each damage state were given in FEMA (2003).

The structural responses evaluated by the structural analysis simulator also are used by the component damage simulator to evaluate the damage state of each structural and nonstructural component in each building in the community at each time step during the earthquake (for the noncollapsed buildings) based on the fragility curves specified in the FEMA P-58 database (FEMA 2012a). The fragility curves of FEMA P-58 are defined using different engineering demand parameters (EDPs), including interstory drift, floor acceleration, or floor velocity. The seismic fragility functions of all the components in FEMA P-58 are described by a lognormal cumulative distribution function (CDF)

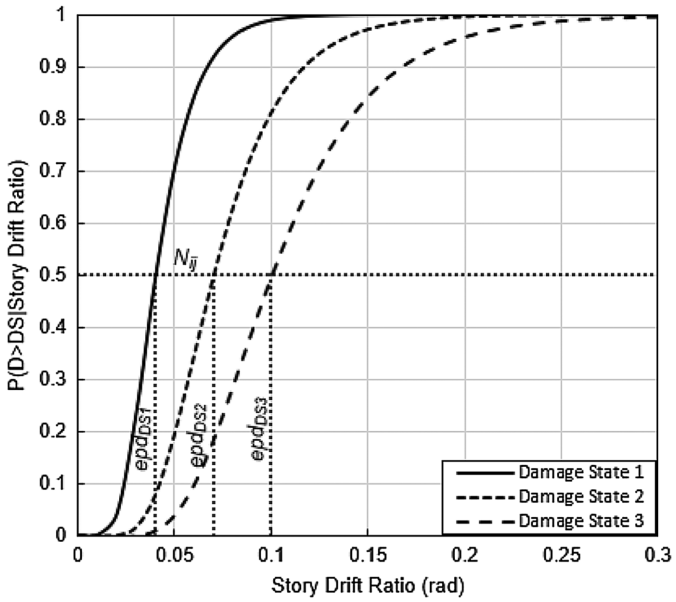

Fig. 3. Fragility curves for steel column base plates specified by FEMA P-58 (B1031.011a).

$$F_R(x) = \Phi\left[\ln\left(\frac{x}{m_R}\right) \Big/ \beta_R\right] \quad (1)$$

where $F_R(x)$ = fragility function; x = EDP; m_R = median capacity; β_R = logarithmic standard deviation; and Φ = standard normal probability integral.

A random number with a uniform distribution between 0 and 1, N_{ij}, is generated at the first time step of the simulation for the jth component of building i. Then the maximum EDP for each damage state is computed using Eq. (1) (Fig. 3). The expected damage state of the jth component of building i is evaluated at each time step during the earthquake for each of the conducted simulations based on the structural response EDP_{ij}, using the following criteria:

$$\begin{aligned}
&\text{No damage if } \text{EDP}_{ij} < \text{EDP}_{DS1}\\
&\text{Damage state 1 if } \text{EDP}_{DS1} \le \text{EDP}_{ij} < \text{EDP}_{DS2}\\
&\text{Damage state 2 if } \text{EDP}_{DS2} \le \text{EDP}_{ij} < \text{EDP}_{DS3}\\
&\text{Damage state 3 if } \text{EDP}_{ij} \ge \text{EDP}_{DS3}
\end{aligned} \quad (2)$$

Seismic Losses

Seismic losses of buildings are classified into two types: economic and social losses. Economic losses are expressed in terms of downtime, repair cost, unsafe placarding status, and amount of debris resulting from damaged components. Social losses are expressed in terms of potential injuries and fatalities resulting from the collapse of buildings or damaged structural and nonstructural components of the buildings. The casualties and debris are evaluated at each time step during the earthquake in the casualties and debris simulators, respectively, whereas the downtime, repair cost, and unsafe placard simulators evaluate the economic seismic losses once, at the end of the earthquake (initial conditions for the recovery stage). The amount of debris generated at each building is calculated based on the empirical approach proposed by the HAZUS methodology (FEMA 2003). The debris is classified into two types: debris that falls in large pieces (e.g., structural elements), and debris that falls in smaller pieces (e.g., bricks, glass, wood, and so forth).

The repair cost and unsafe placarding status of each building in the community are calculated probabilistically using the consequence functions specified in the FEMA P-58 database for all structural and nonstructural components of buildings. The downtime simulator evaluates the downtime of each building in the community using the REDi methodology (Almufti and Willford 2013), which relates the damage state of structural and non-structural components evaluated using FEMA P-58 to actual downtime of buildings including both the repair time evaluated by FEMA P-58 and impeding factors which delay the initiation of repairs to the buildings. The impeding factors considered by the REDi methodology are inspection, financing, contractor mobilization and permitting, and engineering mobilization and review/redesign. These factors typically are evaluated probabilistically and are influenced by the degree of building damage. The downtime simulator constructs an initial repair schedule for each building in the community considering the aforementioned impeding factors, the sequence of repairs that will be undertaken (Fig. 4), the number of workers required to perform repairs of each component type in the building and the maximum number of workers that are able to work on-site simultaneously.

The casualties defined in FEMA P-58 are either fatalities or injuries (requiring hospitalization) that occur inside the building envelope. Minor injuries and outdoor casualties were not considered in the scope of this study. The population distribution in each building is based on its occupancy (i.e., commercial, schools, etc.) as specified in FEMA P-58. Thus, the time of day and day of the

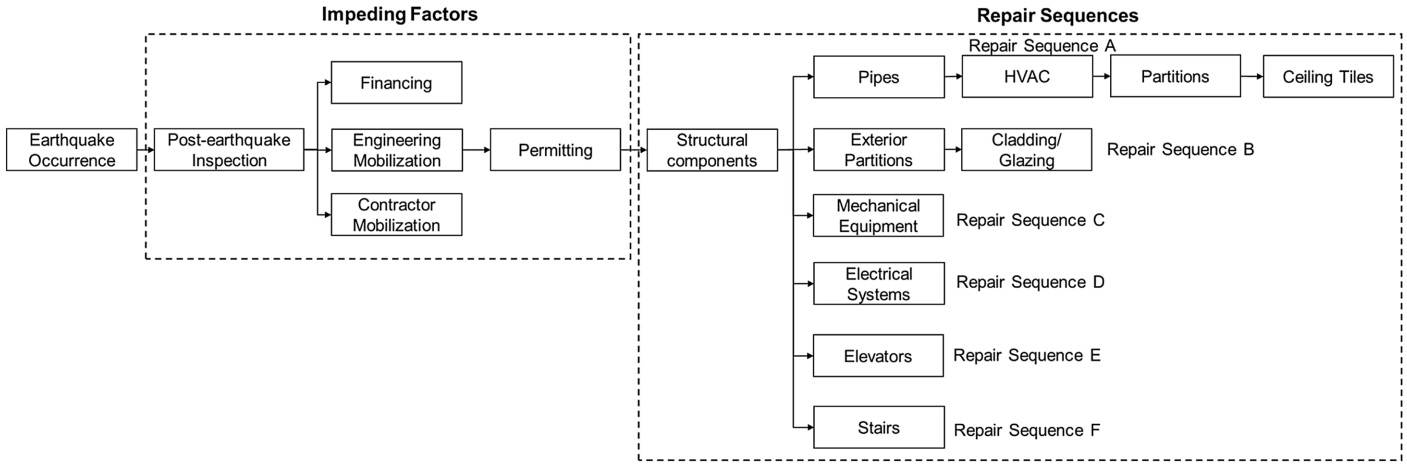

Fig. 4. Repair schedule of buildings including impeding factors proposed in the REDi methodology. (Data from Almufti and Willford 2013.)

Nat. Hazards Rev., 2020, 21(4): 04020041

week of the occurrence of the earthquake are important to accurately evaluate the casualties. In the case of building collapse, the number of injuries and fatalities is calculated based on the casualty rates specified in HAZUS for Casualty severity levels 3 and 4, respectively, and the population present in the building at the time of the earthquake. Casualty severity level 3 is a life-threating injury that requires hospitalization, whereas Level 4 is a fatality. If collapse does not occur, the number of injuries and fatalities at each time step during the earthquake is calculated probabilistically using the consequence functions specified in the FEMA P-58 database, in which each damage state of the structural and nonstructural components includes a description of potential life safety hazards and the corresponding affected area.

Physical Recovery

It is important to differentiate between two types of community recovery efforts: physical and social. Physical recovery is defined as the ability of buildings to recover from the physical damage caused by the earthquake and return back to full functionality. Social recovery is defined in this work as the ability of injured people to return to normal health. In the proposed simulation model, each type of recovery is simulated by different simulators based on the factors affecting the recovery process.

The first step in simulating the physical recovery of a community is to evaluate the initial functionality of each building in the community immediately after the earthquake. Therefore, the components of the buildings are classified into three groups based on their importance and effect on the functionality of the building: (1) structural components (S), (2) nonstructural essential components (NE), and (3) nonstructural nonessential components (NN). The first group (S) is the components that directly affect the stability of the building (e.g., columns, beams, connections, and so forth). The second group (NE) is those components that impede reoccupying a building, i.e., Sequences B, C, D, and F, and pipes from Sequence A defined in the REDi repair sequences (Fig. 4). The third group (NN) is components that do not prevent reoccupancy of the building, i.e., Sequence A, except pipes, and Sequence E defined in the REDi repair sequences.

The damage states of structural and nonstructural components in FEMA P-58 are expressed in discrete states, which are not the same for all components (e.g., bolted shear tabs have three damage states, whereas concrete roof tiles have only two damage states). To relate the DS of the different components of the building to the functionality of the building, it is important to have a unified scale to express the damage of the components. Thus, the repair time required to recover from each DS of the components is normalized to the repair time required to recover from the maximum damage state of the component (designated %RT). Then, Eq. (3) is used to map the DS of the components to a unified scale of three damage states. The limits in Eq. (3) are based on the average %RT considering each DS for components that can be classified into three different damage states according to FEMA P-58 (FEMA 2012a)

$$\begin{aligned} &\text{DS1: } 0 < \%\text{RT} \le 30 \\ &\text{DS2: } 30 < \%\text{RT} \le 75 \\ &\text{DS3: } 100 < \%\text{RT} \le 100 \end{aligned} \tag{3}$$

Four functionality states of a building are considered: (1) not functional (NF), (2) reoccupancy (RO), (3) basic functionality (BF), and (4) full functionality (FF). NF implies that the building suffers from extensive structural or nonstructural damage that threatens life safety. A NF state prevents the building from providing its intended service. The RO state implies that the building suffers from minor to moderate structural or nonstructural damage that does not prevent the occupation of the building. However, RO prevents the building from providing its full intended service. The BF state implies that the building suffers from slight structural or nonstructural damage that does not prevent it from providing its essential intended services. However, the building does not provide its full intended services as it did before the occurrence of the earthquake due to the ongoing repairs that partially hinder this ability. The FF state implies that the building does not suffer any damage after the earthquake, and it can provide its full intended service as it did before the occurrence of the earthquake. To quantify the seismic resilience of the community, each physical functionality state, $Q_p(t)$, is quantified as 0%, 50%, 80%, or 100% for the NF, RO, BF, or FF states, respectively, based on the definition of each functionality state described previously. The initial functionality of each building in the community is related to the level of damage of the three aforementioned components (S, NE, and NN) in the physical recovery simulator using the combinations in Fig. 5.

The available resources simulator evaluates the available number of workers in the community at each time step during the recovery stage based on the number of casualties obtained from the healthcare system simulator. It is assumed that the percentage of total casualties in the population of the community is the same as the percentage of casualties in the population of workers. Thus, the available number of workers increases during the simulation due to recovery of workers from earthquake-induced injuries. The physical recovery simulator allocates the limited number of workers available in the community calculated by the available resources simulator to repair the damaged buildings using the repair schedule and required number of workers evaluated by the downtime simulator. The number of workers is allocated to buildings based on the priority of the building in the community in which the buildings are prioritized based on their usage and occupancy level. Usage priority used in this research is as follows: hospitals, schools, residential houses, commercial buildings, retail, and other occupancies.

After allocating the available workers to repair the damaged buildings in the community, the physical recovery simulator returns a list of buildings that have not been repaired at the current time step, due to the limited number of available workers, to the downtime simulator to update their repair schedule. The downtime simulator sends back the updated schedules to the physical recovery simulator to be used in the next time step.

The physical functionality of each building in the community is updated at each time step during the recovery stage based on the functionality in the previous step and the damage state of different components in the building. For a building in the NF state, the physical functionality is restored in two stages. The first stage is to return to the RO state after finishing the repairs of the components specified as Schedules B, C, D, and F, and pipes from Sequence A in the REDi methodology. The repair sequence of the different components adopted in the REDi methodology is summarized in Fig. 4. The second stage is to return to the FF state after finishing all the required repairs in the building. However, for a building in the RO or BF state, the physical functionality is restored in only one stage by returning to the FF state after finishing all the repairs in the building. Fig. 6 is a schematic diagram of the physical functionality restoration process. The total physical functionality of the community $Q_p(t)$ is evaluated at each time step during the recovery stage as the weighted average of all the physical functionalities of the buildings in the community at this time step based on the importance of each building in the community as follows:

$$\%Q_p(t) = \frac{\sum_{i=1}^{n} I_i \times \%Q_i(t)}{\sum_{i=1}^{n} I_i} \quad (4)$$

where $\%Q_i(t)$ = functionality of building i in community at time step t; I_i = seismic importance factor of building i based on its occupancy as specified in ASCE 7-16 (ASCE 2016); and n = total number of buildings in community.

Social Recovery

The social recovery of the community is a measure of the number of casualties in the community with respect to the total population. Therefore, the first step to simulate social recovery of the community is to evaluate the number of injuries that need treatment at each time step during the recovery stage. At the end of the earthquake (i.e., the initial time step of the recovery stage), the casualties simulator evaluates the total number of injuries and fatalities at each building in the community. Some of the injured will be trapped in damaged or collapsed buildings (i.e., they cannot be assigned to hospitals until they are rescued). In the proposed model, 60% of the injured people are assumed to be trapped and to need rescue during the recovery stage, as modeled by Fawcett and Oliveira (2000). The rate at which the trapped, injured people are rescued during the recovery stage depends on the emergency response capabilities of the community and is an important characteristic of resilient communities. In the proposed simulation model, the daily rate of rescue of injured people is assumed to be constant. However, it can be adapted to any other assumption, as discussed by Fawcett and Oliveira (2000). The other 40% of injured people will be waiting to receive treatment by the hospital system in the community. The healthcare system simulator assigns the waiting injured people to hospitals in the community based on the closest hospital to the building in which the injury occurs and the available number of beds in the hospital, which is calculated as follows:

$$B(t) = Q_p(t) \times B_t - B_b(t) \quad (5)$$

where $B(t)$ = available number of beds at time t during recovery stage; $Q_p(t)$ = physical functionality of hospital building evaluated by the physical recovery simulator; B_t = total number of beds in hospital before the earthquake; and $B_b(t)$ = number of filled beds at time t.

The length of stay for an injured person in the hospital to receive treatment is modeled as a random variable with lognormal distribution with a median of 13 days and dispersion of 0.4. These numbers are based on data regarding postearthquake injuries treated at a field hospital after the Haiti earthquake in 2010 (Nos 2011). During the first days after the earthquake, there is a high mortality rate, which is about 20%–25% according to Coupland (1994). The proposed simulation model considers a constant mortality rate of 3% per day for untreated injuries, as modeled by Fawcett and Oliveira (2000). The remaining 97% of untreated injured people will continue to the next time step to be assigned to hospitals if open beds are available.

Rescued people with injuries are added to the waiting injured to be assigned to hospitals in the next time step. Furthermore, it is assumed that 20% of the waiting injured people who are not assigned to hospitals at the current time step will be mobilized to hospitals in nearby zones to model the fact that injured people usually are distributed to nearby health care facilities after a seismic event in cases in which no beds are available in the hospitals in their zone. Fig. 7 is a schematic diagram of the injury-treatment process during the recovery stage performed in the healthcare system simulator. The social functionality of the community is evaluated at each time step during the recovery stage by the social recovery simulator as follows:

$$\%Q_s(t) = 100 \times \left(1 - \sum_{i=1}^{n} C_i(t)/P\right) \quad (6)$$

where $C_i(t)$ = total number of injuries and fatalities at building i at time step t; and P = total population in the community. The social functionality of the community will not return to 100% if fatalities occur.

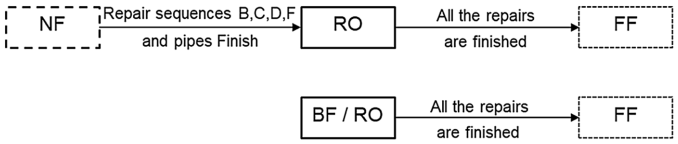

Fig. 6. Restoration of building functionality at each time step during the recovery stage.

Quantifying Seismic Resilience of Communities

The total functionality of the community is calculated at each time step during the recovery stage by the total recovery simulator as the product of the physical and social functionalities as follows:

$$\%Q_t(t) = Q_p(t) \times Q_s(t) \quad (7)$$

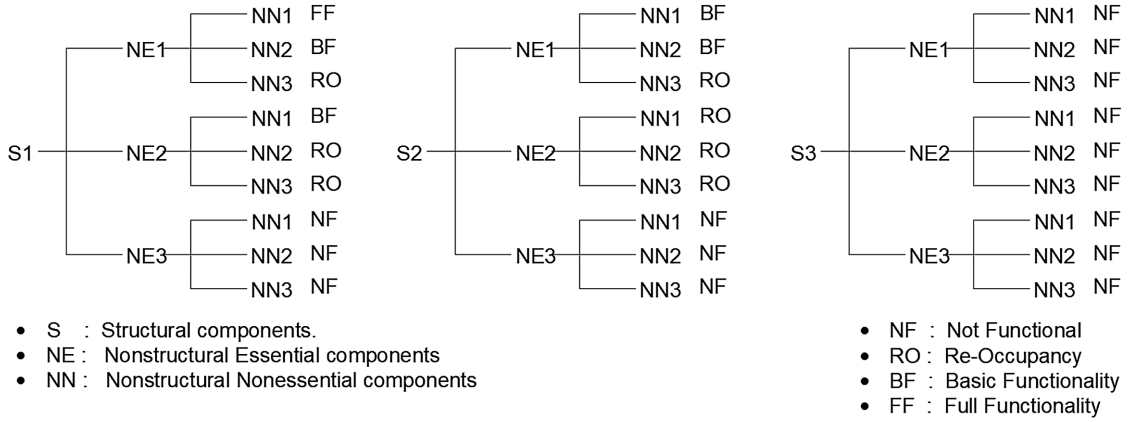

Fig. 5. Combinations used to evaluate the initial functionality of buildings in the physical recovery simulator (the appended number is the damage state).

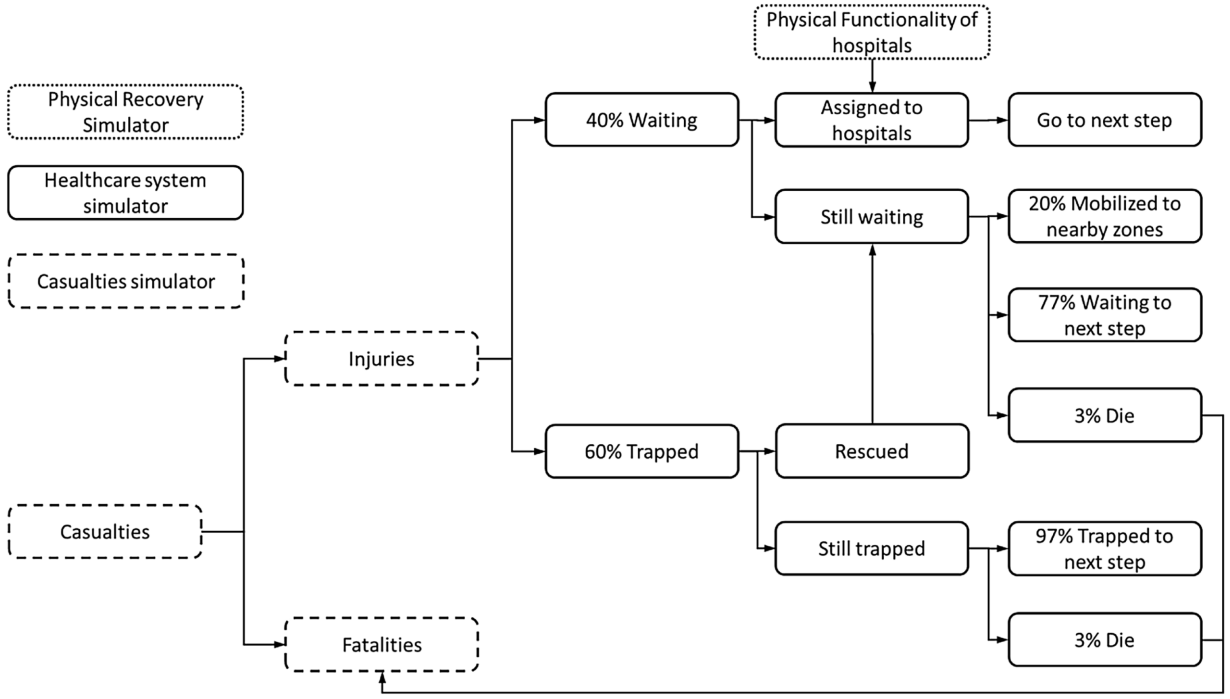

Fig. 7. Schematic diagram for the injury treatment process performed in the healthcare system simulator.

The seismic resilience index of the community ($\%R$) is evaluated as the area under the total recovery path during the recovery time (Fig. 8), which can be represented mathematically as follows (Bruneau and Reinhorn 2004, 2007):

$$\%R = \frac{\int_{t_{oE}}^{t_0+T_{\mathrm{RE}}} Q_t(t)}{T_{\mathrm{RE}}} \tag{8}$$

where t = time during recovery stage; t_{oE} = time when earthquake occurs; T_{RE} = time required by community to restore full functionality after the earthquake; and $Q_t(t)$ = total functionality of the community calculated by Eq. (7).

Case Study: Seismic Resilience of Archetype Community

Building Portfolio

The proposed simulation model and its capabilities are demonstrated through a case study that focused on a part of Shelby County, Tennessee (Fig. 9). It is a typical midsize community with a population of approximately 40,000 (Statistical Atlas 2018), and is approximately 14 km^2 (5.4 mi^2) in area. It consists of about 8,600 buildings with different occupancies, structural systems, heights, and design codes. The data for the buildings were extracted from the database provided in Ergo-EQ software version 4.0 Beta 2 (NCSA 2018). The buildings were mapped to 100 different developed archetype buildings. Table 2 lists the archetype buildings designated according to the naming scheme described previously and the total number of each archetype. Most of the buildings were wooden houses that are typical of US communities.

There were three hospitals that were 2, 4, and 12 stories high (SFA-2-5, SFA-4-5, and CSA-12-5, respectively). The total number of beds in the hospitals before the earthquake was 140, 223, and 326 for SFA-2-5, SFA-4-5, and CSA-12-5, respectively, based on data for hospitals located in Tennessee from the AHD (2018). The total number of construction workers available in the community before the earthquake was 1,400, which was approximately 3.5% of the community's population, representing the same percentage of construction workers in the US population as per data from the BLS (2018). The buildings were prioritized as mentioned previously and the buildings with the same priority were repaired starting from the Midtown area (north side of the community).

Moment-resisting and braced-frame steel structures were assumed to be the same as the archetype buildings designed in NIST (2010). The seismic demands on the moment-resisting frame buildings were assumed to be resisted by the three-bay special moment frames (SMFs) on the buildings' perimeter. The behavior of the moment-resisting frame buildings was modeled using 2D concentrated plasticity beam–column elements in OpenSees (McKenna et al. 2000). The modified Ibarra–Medina–Krawinkler deterioration model (Ibarra and Krawinkler 2005) was used to represent the

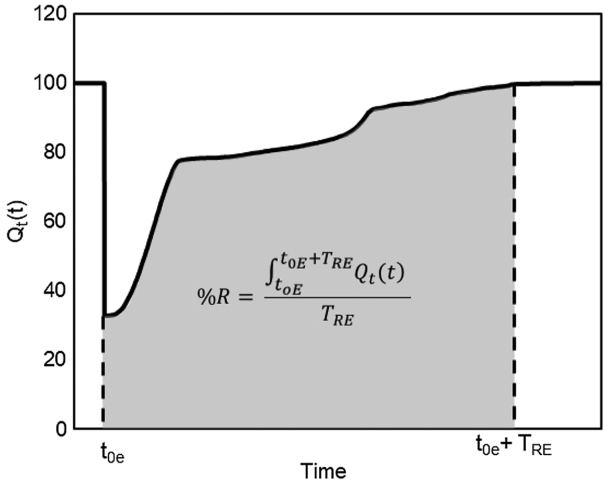

Fig. 8. Evaluation of seismic resilience of a community.

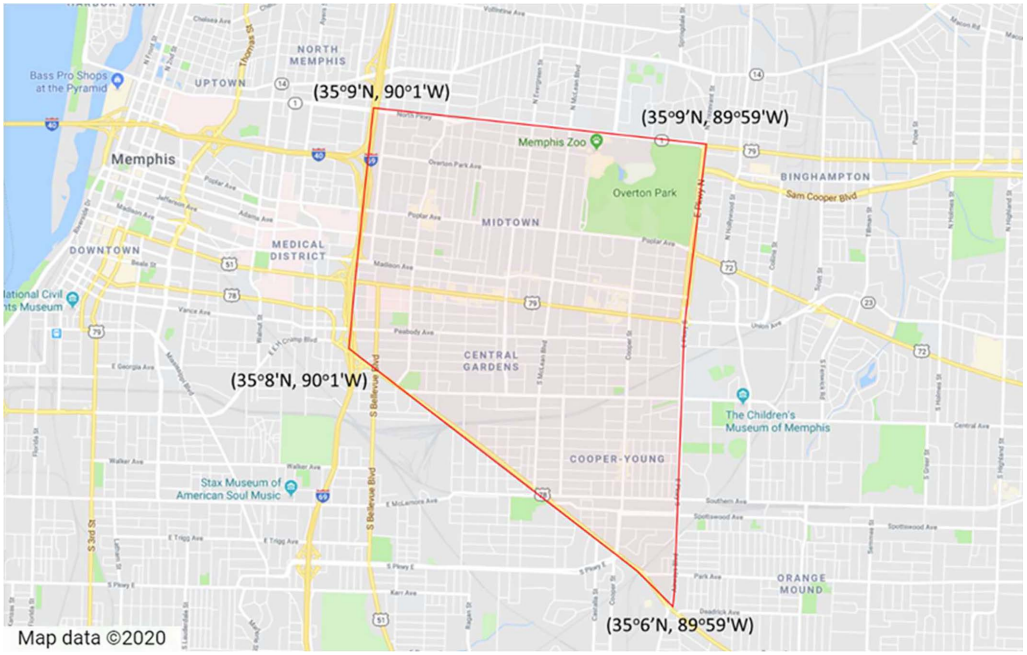

Fig. 9. Archetype community location. (Map data ©2020 Google.)

Table 2. List of building archetypes and total number of each archetype in studied community

Model	Total	Model	Total	Model	Total	Model	Total	Model	Total
CFB-2-1	2	CSC-20-1	1	RMC-2-2	1	SFC-2-1	5	WLC-2-9	5
CFB-2-10	1	CSC-20-8	1	RMC-2-7	1	SFC-4-1	1	WLC-2-7	177
CFB-2-9	4	CSC-2-1	1	RMC-2-9	3	URMB-2-7	1	WLC-3-1	4
CFB-6-1	2	CSC-2-2	1	SBA-2-1	1	URMC-2-6	1	WLC-3-7	2
CFB-8-1	1	CSC-2-7	1	SBA-2-10	14	URMC-2-1	220	WSA-1-7	11
CFC-12-10	1	CSC-2-9	4	SBA-2-9	2	URMC-2-7	105	WSA-2-7	93
CFC-12-7	1	CSC-4-2	3	SBA-4-9	5	URMC-2-10	60	WSA-3-7	209
CFC-2-1	7	CSC-4-7	2	SBB-2-1	1	URMC-2-2	1	WSB-1-1	1
CFC-2-10	4	CSC-6-1	1	SBB-2-10	9	URMC-2-9	64	WSB-1-10	8
CFC-2-7	29	CSC-6-7	1	SBB-2-9	7	URMC-4-7	139	WSB-1-7	1
CFC-2-9	2	CSC-8-1	1	SBC-2-1	8	URMC-4-10	15	WSB-1-9	60
CFC-4-1	3	CSC-8-7	3	SBC-2-10	51	URMC-4-2	4	WSB-2-7	3
CFC-4-7	1	RMA-2-1	1	SBC-2-9	8	URMC-4-1	2	WSC-1-9	172
CFC-6-1	1	RMA-2-7	3	SBC-4-1	40	URMC-4-9	6	WSC-1-10	25
CFC-6-7	2	RMA-2-9	2	SBC-4-10	6	URMC-6-1	11	WSC-1-1	1
CFC-8-7	1	RMA-4-1	10	SBC-4-9	4	URMC-6-10	1	WSC-1-7	4,671
CSA-12-5	1	RMB-2-1	1	SFA-2-5	1	WLA-2-7	2	WSC-2-1	5
CSA-2-9	1	RMB-2-9	2	SFA-4-5	1	WLB-2-1	3	WSC-2-9	1
CSB-20-1	1	RMB-4-1	11	SFB-2-1	1	WLB-2-7	4	WSC-2-7	2,156
CSC-12-7	2	RMC-2-1	1	SFB-2-7	1	WLC-2-1	4	WSC-3-7	1

strength and stiffness deterioration properties due to cyclic loading, in which the material model parameters were quantified using the experimental database of Lignos and Krawinkler (2012).

The seismic demands on the braced-frame buildings were assumed to be resisted by one-bay special concentrically braced frames (SCBF) located on the buildings' perimeters. The behavior of the SCBFs was modeled using 2D concentrated plasticity models (McKenna et al. 2000) in OpenSees. Due to its modular nature, the proposed simulation model supports the use of detailed structural models of all of the buildings in the inventory. However, for the sake of simplicity and to showcase the ability of the proposed simulation model to accommodate different modeling methods of the buildings in the community, the other types of buildings were represented using the fragility curves provided in HAZUS (FEMA 2003). The Normative Quantity Estimation Tool provided in Volume 3 of FEMA P-58 (FEMA 2012a) was used to evaluate the nonstructural component quantities and distributions in the buildings. This tool estimates the quantities of the components likely to be in a building with a specific occupancy on a gross square-foot basis.

Seismic Hazard

The seismic event was the first horizontal component of the ground motion record RSN 1961 (PEER 2018) which was recorded at the Lepanto station near the studied community. The epicenter was located at 35°18′N, 90°18′W, and the peak ground acceleration (PGA)

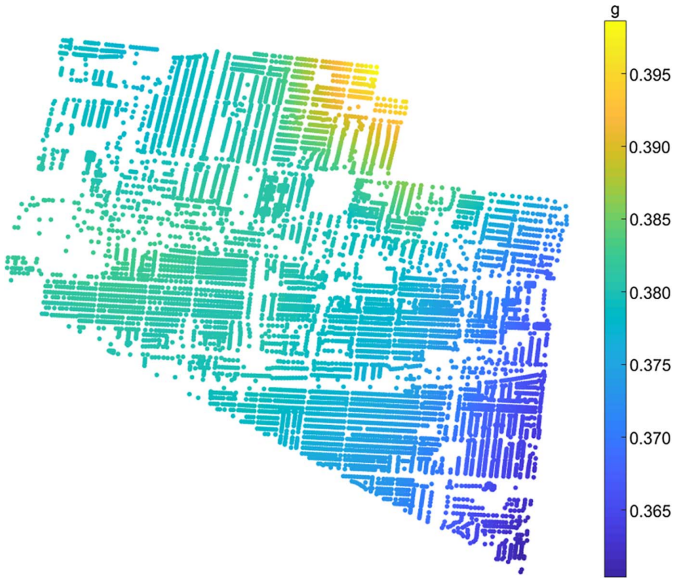

Fig. 10. Spatial distribution of the PGA at the buildings location in the studied community.

was scaled at each building location to meet the PGA for a M_w7.7 earthquake scenario specified by the USGS (2018) for the studied region. The spatial distribution of the PGA at the buildings location in the studied community is shown in Fig. 10. The earthquake event was assumed to occur on a weekday at 8:00 p.m. For the sake of simplicity, vertical propagation of the ground motion was not considered in the demonstrated case study.

Results and Discussion

To account for the many uncertainties inherent in the factors affecting the different types of losses after a seismic event, the FEMA P-58 methodology (FEMA 2012a) and thus the proposed model uses a Monte Carlo procedure to perform loss calculations. The proposed simulation model is computationally demanding and therefore was implemented and run within a parallel computing environment. The computational time for running 100 Monte Carlo simulations for the presented case study was about 10 h on a personal computer with four cores and 32 GB RAM. The number of Monte Carlo simulations was selected based on a sensitivity study in which the number of simulations progressively increased until convergence occurred (after 150 simulations). Convergence was deemed to occur when changes in the range, mean, and standard deviation of the recovery time (T_{RE}) and resilience index (%R) did not exceed 10%. The sampling was performed based on the distribution properties of each component specified in the FEMA P-58 methodology (FEMA 2012b). Fig. 11 shows the evolution of trapped and free individuals with injuries during the earthquake for an arbitrary Monte Carlo simulation in two areas of the studied community, namely Midtown and Central Gardens (Fig. 9). No injuries occurred in either areas during the first few seconds. However, by 30 s into the simulation, about 150 people were trapped and had injuries in Midtown. By 60 s, the number increased to 1,100. Dynamic analysis implemented in the proposed simulation model provides step-by-step information about injuries, which can help rescue and medical teams better plan their first response efforts during simulation exercises. For longer-duration events (such as hurricanes), in which actual models are being used during the event itself, data of this sort can be used to optimize first-response operations, emphasizing the importance of dynamic analysis.

Most of the buildings were in the none to moderate damage states (75.6%), which indicates that the studied community performed relatively well under the seismic event. About 9.5% of the buildings suffered complete collapse. Table 3 lists the mean percentage of collapsed buildings with respect to building material, design code, and building occupancy. Most of the collapsed buildings were wood buildings (67.1%), which represented the majority of the buildings in the studied community. No steel buildings collapsed during the studied earthquake, whereas 3.2% of the collapsed buildings were RC buildings. Almost all the collapsed buildings were those designed according to old codes (pre-1973 buildings) emphasizing the relatively high vulnerability of older, unretrofitted buildings in modern communities. Most of the collapsed buildings were residential buildings, which represented the majority of the building inventory.

The majority of the casualties associated with earthquakes result from the collapse of buildings. As reported by Nobuhara et al. (2000), about 90% of the casualties that resulted from the 1995 Kobe earthquake were due to collapsed buildings. This is in accord with the results of the proposed model, in which 93% of the casualties in the studied community occurred in collapsed buildings, whereas the other 7% were caused by falling components inside

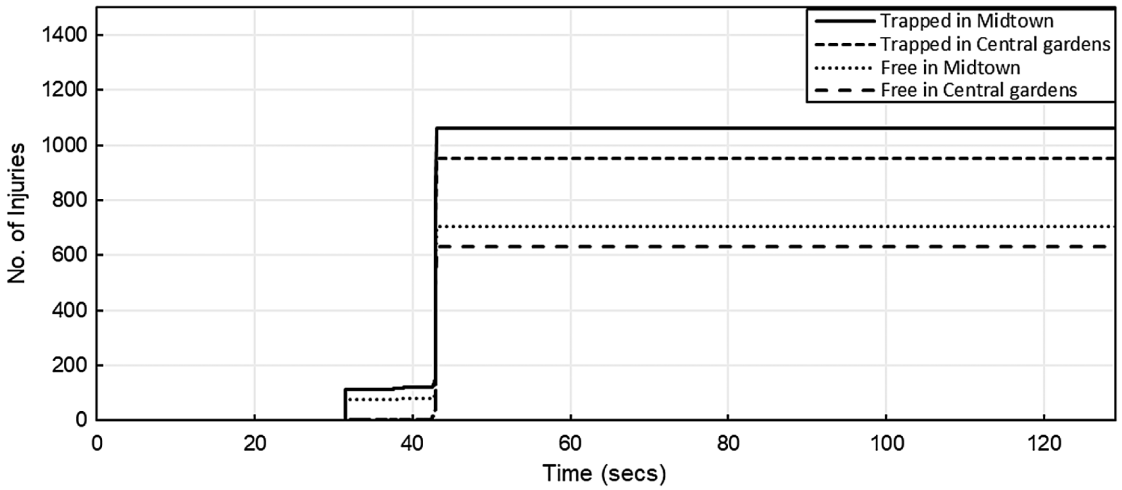

Fig. 11. Evolution of trapped and free injuries during the earthquake for an arbitrary Monte Carlo simulation in two areas of the studied community.

Table 3. Distribution of building collapse and casualties with respect to building characteristics in studied community

Building attribute	Building characteristics	Collapsed buildings (%)[a]	Casualties (%)[b]
Building material	RC	26 (3.2)	715 (19.1)
	Reinforced masonry	3 (0.4)	22 (0.6)
	Unreinforced masonry	239 (29.3)	655 (17.5)
	Wood	546 (67.1)	2,352 (62.8)
Design code	New (Code A)	2 (0.2)	11 (0.3)
	Moderate (Code B)	9 (1.1)	82 (2.2)
	Old (Code C)	803 (98.7)	3,651 (97.5)
Building occupancy	Commercial	56 (6.9)	15 (0.4)
	Residential	670 (82.4)	3,426 (91.5)
	Retail	61 (7.5)	300 (8.0)
	Warehouse	27 (3.2)	3 (0.1)

[a]Numbers without parenthesis are the number of buildings. Whereas, the numbers with parenthesis are their percentages in the community (%).
[b]Numbers without parenthesis are the number of casualties. Whereas, the numbers with parenthesis are their percentages in the community (%).

the noncollapsed buildings. The percentage of casualties in RC buildings was relatively high compared with that in wood buildings (Table 3). Approximately 98% of the casualties occurred in buildings designed according to old codes (pre-1973 buildings), again emphasizing the higher vulnerability of older, unretrofitted buildings in modern communities. As noted previously, the earthquake event was assumed to occur on a weekday at 8:00 p.m., which implies that most of the population was in residential buildings rather than other types of buildings. Consequently, most of the casualties (91.5%) were located in residential buildings.

Fig. 12 shows the spatial distribution of the physical functionality of the buildings during the recovery stage immediately after the earthquake and at three different times for one arbitrary Monte Carlo simulation. A significant number of buildings regained their functionality in the first 60 weeks (~1.2 years) after the earthquake. This relatively rapid recovery in functionality is attributed to the fact that buildings with high repair priority and lower damage states have relatively low delay time. However, after the first 60 weeks, repair of the buildings with lower priority and higher damage states (thus requiring longer repair times) started, contributing to the plateau in the recovery trajectory in Fig. 13(a). The mean restoration period of full physical functionality for the studied community, T_{RE}, was approximately 240 weeks (~4.6 years). The recovery clouds in Fig. 13(a) show the range of possible recovery trajectories, taking into consideration the inherent uncertainties in the proposed methodology. To improve the recovery of the studied community in response to earthquakes, several mitigation actions were considered and evaluated, as discussed subsequently.

Evolution of the social functionality of the studied community is shown in Fig. 13(b). During the first few weeks, the mean number of treated injuries in the local hospitals was relatively low

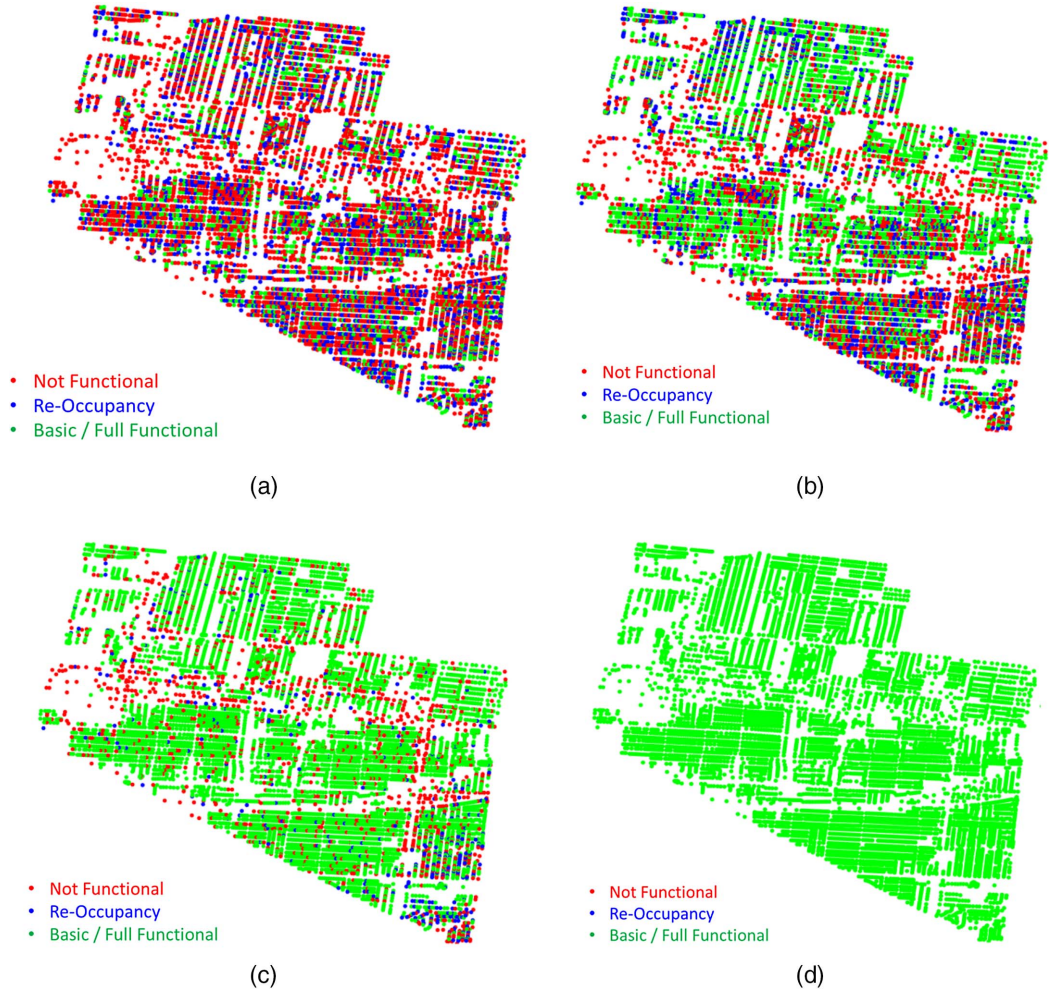

Fig. 12. Spatial distribution of the functionality of the buildings in the studied community for one arbitrary Monte Carlo simulation: (a) immediately after the earthquake; (b) after 30 weeks; (c) after 60 weeks; and (d) after 240 weeks.

Nat. Hazards Rev., 2020, 21(4): 04020041

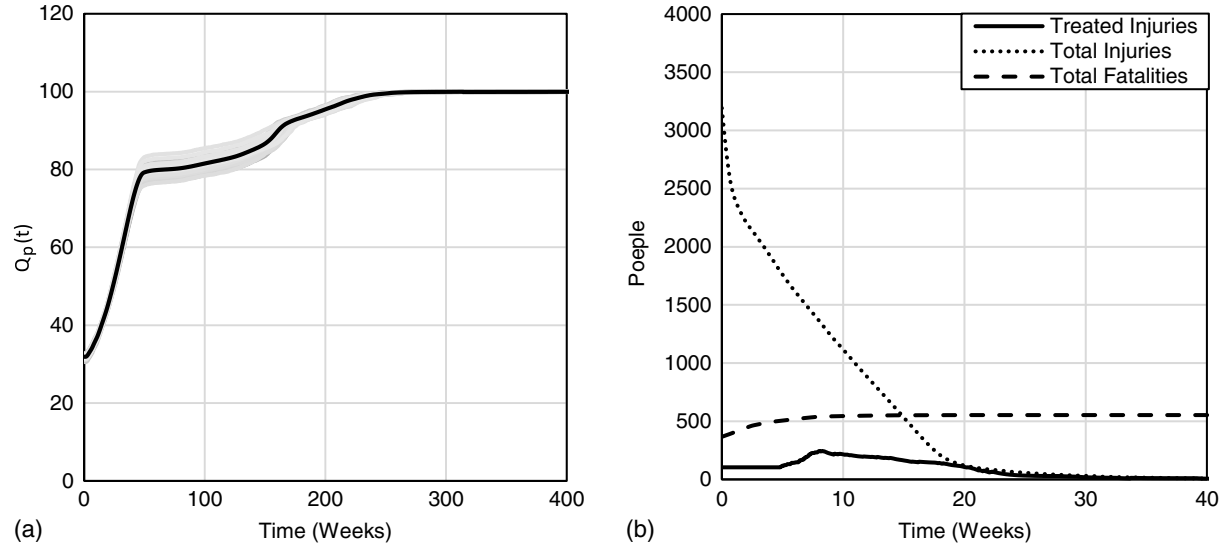

Fig. 13. (a) Physical recovery trajectories for conducted Monte Carlo simulations and the mean recovery trajectory for the studied community (shaded area represents the recovery clouds); and (b) mean number of casualties versus time during the recovery stage of the studied community.

(approximately 120 injuries) because of the loss of functionality of the hospitals due to physical damage. However, as time progressed, the hospitals regained their functionality and the mean number of treated injuries increased gradually to 240 injuries. After that, patients with injuries started to regain their health and leave the hospitals, allowing others to receive treatment. Thus, the mean number of treated injuries decreased gradually until it reached 0 at 30 weeks after the earthquake (~7 months). In addition, Fig. 13(b) shows the evolution of the total injuries in the studied zone during the recovery stage. The decrease in the first few weeks was due to the 20% untreated injuries sent to nearby zones, as discussed previously. The number of fatalities increased during the first 7 weeks from 300 fatalities immediately after the earthquake to over 500 because of the daily mortality rate of untreated injuries, as discussed previously.

A key design feature of the proposed simulation model is that it operates in a plug-and-play sense to facilitate studying the effects of interdependencies between the different systems of the community. To showcase this important capability, Fig. 14 plots the mean total recovery trajectory of the community without considering the interdependency between physical recovery and available number of workers in the community. This simulation was achieved by simply unplugging the available resources simulator from the model (no interdependency) compared with the normal case in which all the interdependencies were considered (interdependency). Considering the interdependency between the physical recovery and available number of workers in the community delayed the recovery of the community and shifted the recovery trajectory to the right, which reduced the resilience index of the community from 90% to 81% (10% reduction). This reduction in the community resilience index is demonstrated by the shaded area under the recovery trajectory in Fig. 14. A fixed time frame must be used in Eq. (8) to be able to use the computed community resilience index ($\%R$) as a metric to compare resilience for different cases. Thus, T_{RE} in Eq. (8) is the maximum recovery time between the two compared trajectories (i.e., 240 weeks). In addition, the mean restoration period of full functionality for the community, T_{RE}, decreased from 240 weeks (~4.6 years) when considering the interdependency to only 150 weeks (~2.9 years) when neglecting the interdependency, which is a substantial difference in recovery time (~38%).

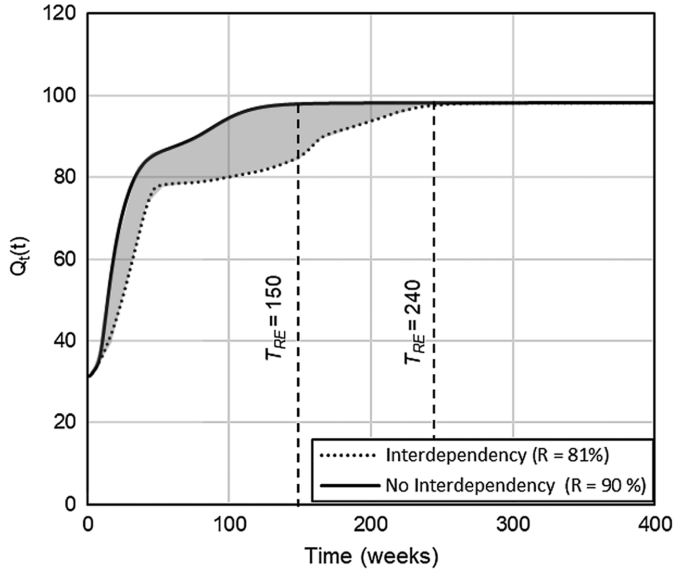

Fig. 14. Effect of the interdependency between physical recovery and availability of resources in the community during the recovery stage.

Effectiveness of Hazard Mitigation Plans

To further demonstrate the capability of the proposed simulation model to support hazard mitigation planning, a sensitivity study was performed to examine the effect of prehazard and posthazard mitigation actions on the response of the studied community to earthquakes. Prehazard mitigation actions are defined as those taken before an extreme event to mitigate the effect of the hazard. Posthazard mitigation actions are those taken at certain times during the recovery process to provide a better recovery trajectory. Accordingly, three mitigation actions were considered in this study and applied to the studied community through the proposed model. The selected actions are representative of a multitude of actions that could be taken and were used to showcase the capability of the developed simulation model.

- Action A: a prehazard mitigation action through a community-wide residential building retrofit plan that entails upgrading the

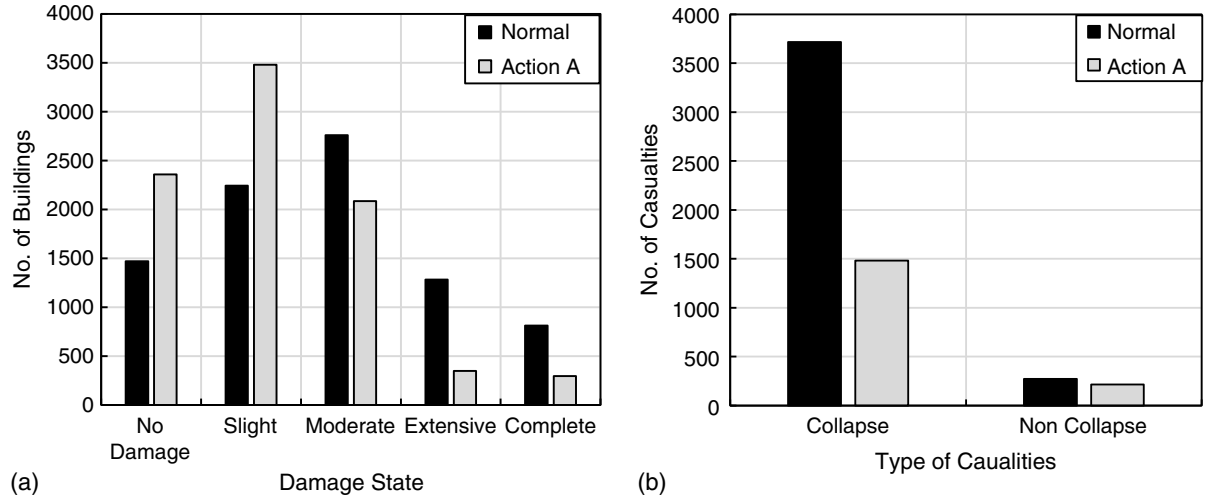

Fig. 15. Effect of mitigation Action A on (a) mean number of buildings in different damage states; and (b) mean number of casualties resulting from collapsed and noncollapsed buildings.

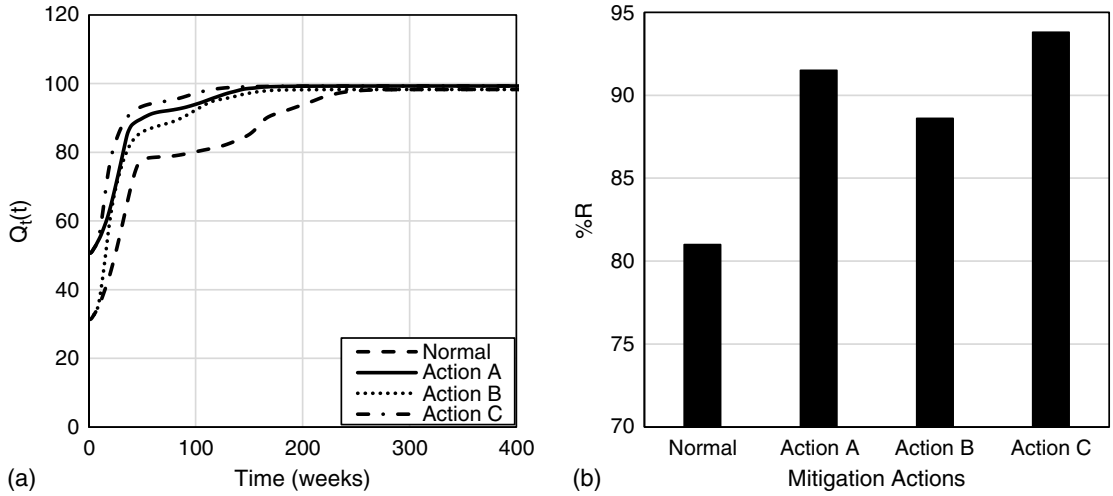

Fig. 16. Effect of the proposed mitigation actions on (a) recovery trajectory of the studied community; and (b) resilience index (%R) of the studied community.

seismic resistance of all residential buildings that were built according to design codes prior to 1973 (Code C buildings) to a current design level (Code A buildings);

- Action B: a posthazard mitigation action that entails increasing the number of workers to 3,000 (i.e., requesting more workers from a nearby state) starting 2 months (60 days) after the earthquake; and
- Action C: both Actions A and B.

Fig. 15(a) shows the mean number of buildings in different damage states under normal conditions and after applying Action A. Upgrading the seismic design of residential buildings reduced the mean number of collapsed buildings from 814 to 298 collapsed buildings (64% reduction). The mean number of buildings in the none to moderate damage states increased from 6,473 to 7,921 buildings (22% increase). The mean number of collapse-related casualties decreased significantly from 3,700 to 1,500 (a 59% reduction) [Fig. 15(b)]. Clearly, Action A is quite effective in reducing earthquake losses.

Fig. 16(a) plots the mean total recovery trajectory of the studied community before and after applying the mitigation actions. With Action A, the initial total functionality of the community immediately after the earthquake increased significantly from 31% to 50%. The mean restoration period to maximum total functionality, T_{RE}, decreased from 240 weeks (~4.6 years) to 160 weeks (~3.0 years). Applying Action B did not affect the initial total functionality of the community immediately after the earthquake. However, the mean restoration period to maximum total functionality, T_{RE}, decreased from 240 weeks (~4.6 years) to 170 weeks (~3.2 years). Action C increased the initial total functionality and decreased the mean restoration period to maximum total functionality for the studied community, T_{RE}, from 240 weeks (~4.6 years) to 120 weeks (~2.3 years), which was the best among all the considered mitigation actions.

Fig. 16(b) shows the resilience index (%R) for different cases of the studied community. The recovery time, T_{RE}, used in Eq. (8) to evaluate %R is the maximum recovery time between the compared

trajectories, as discussed previously (i.e., 240 weeks). Applying the pre- and posthazard mitigation actions improved the resilience of the studied community. Action A increased $\%R$ from 81% to 92% a 13% improvement in community resilience. Action B increased $\%R$ from 81% to 89%, a 9% improvement in community resilience. Action C increased $\%R$ from 81% to 94%, a 16% improvement in community resilience.

Choosing the appropriate mitigation strategy depends on many factors which are community-specific, beyond just the resilience index ($\%R$). One of these factors is the initial investment required for each plan (e.g., the cost of upgrading the design of current buildings versus repairing them after a seismic event). Another factor is the social aspect of the problem. For example, Action B provides a comparable enhancement to that of Action A in regard to the resilience index ($\%R$) of the community. However, it produces more casualties than Action A, which may motivate decision makers to choose Action A or Action C.

Simulation Model Limitations

Although the proposed simulation model combines the physical aspect of community resilience (related to the buildings) and the social aspect (related to the injuries/fatalities), other critical dimensions of community resilience were been accounted for in this study. For example, bridge and transportation network damage can affect traffic flow and, therefore, access to healthcare facilities. Lifelines, such as power, gas, and water systems, also can profoundly influence resilience and the recovery trajectory. Furthermore, the social vulnerability is expressed in terms of injuries and fatalities only. However, there are other short- and long-term social vulnerability indicators that affect the resilience of communities, including relocation, business disruption, job loss, supply disruption, family stress, and neighbor disruption that are out of scope of the current study. These aspects of community resilience can be accounted for in the future through the addition of relevant simulators. Furthermore, the presented results and mitigation strategies were based on the assumptions discussed previously related to the building portfolio, components, and ground motion scenario. Clearly, the results (i.e., building collapse, injuries, and recovery outcomes) will change when using different points for fault rupture or a different city. However, the proposed model allows for the ability to evaluate multiple scenarios and strategies, providing the necessary data to make informed decisions.

Summary and Conclusions

This study proposes a simulation-based model for the assessment and quantification of seismic resilience of communities. The proposed model is modularized into independent simulators, each representing an aspect of the overall problem. The system is designed to step through time as the seismic event occurs (time step in seconds) and as the community recovers after the event (time step in days). Due to its modularized nature, the proposed simulation model can combine two different aspects of community recovery to quantify the seismic resilience of communities: physical and social recovery.

The proposed model was demonstrated through a case study in which a part of Shelby County, Tennessee, was subjected to a M_w7.7 earthquake located northwest of Memphis. The results showed that the physical recovery of the studied community was substantially slower than the social recovery. To demonstrate the capability of the proposed simulation model in supporting hazard mitigation planning, a study was performed to examine the effect of different mitigation strategies on community resilience. Three different mitigation actions were studied and applied through the proposed model. The results of the case study showed that upgrading the seismic resistance of residential buildings to current codes improved the seismic resilience of the studied community by 10%, whereas increasing the number of workers from 1,400 to 3,000 during the recovery stage improved the seismic resilience of the studied community by 7.5%.

The proposed simulation model has a number of key advantages that make it well suited for community resilience computations. First, it provides fine granularity by allowing for separate treatment of each building in the community. Building seismic performance is used to calculate economic and social losses, both of which are handled in an integrated manner within the model. Second, due to its modularized nature, the proposed model is scalable and adaptable. It is designed to operate within a plug-and-play environment and, therefore it facilitates the improvement/substitution of any discipline-specific simulator without affecting the other simulators. Third, the ability to conduct in-event simulation (by explicitly stepping through time) allows for full consideration of the interdependencies that arise between the different systems of society. For instance, without in-event simulation, it is not possible to consider the effect of the physical recovery of the hospitals on social recovery as it pertains to injuries. Increasing the number of workers at a certain time during the recovery stage is straightforward using the current configuration. The proposed simulation model is a key step toward quantifying the seismic resilience of communities based on detailed loss estimation models as well as recovery models that consider the effect of multiple interdependencies between different systems of the community.

Data Availability Statement

All data, models, and code generated or used during the study appear in the published article.

Acknowledgments

This work was supported by the University of Michigan and the US National Science Foundation (NSF) through grant ACI-1638186. Any opinions, findings, conclusions, and recommendations expressed in this paper are those of the authors and do not necessarily reflect the views of the sponsors.

References

Abdelhady, A. U., S.-Y. Lin, L. Xu, O. A. Sediek, A. W. Hlynka, S. El-Tawil, S. M. Spence, J. McCormick, V. R. Kamat, and C. Menassa. 2019. "A distributed computing platform for community resilience estimation." In *Proc., 13th Int. Conf. on Applications of Statistics and Probability in Civil Engineering, ICASP13*. Seoul: Seoul National University Library.

AHD (American Hospital Directory). 2018. "Individual hospital statistics for Tennessee." Accessed August 15, 2018. https://www.ahd.com/states/hospital_TN.html.

Almufti, I., and M. Willford. 2013. *REDi™ rating system: Resilience-based earthquake design initiative for the next generation of buildings*. London: ARUP Group.

ASCE. 2016. *Minimum design loads and associated criteria for buildings and other structures*. ASCE/SEI 7-16. Reston, VA: ASCE.

BLS (Bureau of Labor Statistics). 2018. "Construction: NAICS 23." Accessed August 10, 2018. http://www.bls.gov/iag/tgs/iag23.htm.

Bruneau, M., and A. M. Reinhorn. 2004. "Seismic resilience of communities—Conceptualization and operationalization." In *Proc., Int. Workshop on Performance Based Seismic Design*, edited by P. Fajfar and H. Krawinkler, 161–172. Berkeley, CA: Univ. of California.

Bruneau, M., and A. M. Reinhorn. 2007. "Exploring the concept of seismic resilience for acute care facilities." *Earthquake Spectra* 23 (1): 41–62. https://doi.org/10.1193/1.2431396.

Burton, H. V., G. Deierlein, D. Lallemant, and T. Lin. 2016. "Framework for incorporating probabilistic building performance in the assessment of community seismic resilience." *J. Struct. Eng.* 142 (8): 1–11. https://doi.org/10.1061/(ASCE)ST.1943-541X.0001321.

Burton, H. V., G. Deierlein, D. Lallemant, and Y. Singh. 2017. "Measuring the impact of enhanced building performance on the seismic resilience of a residential community." *Earthquake Spectra* 33 (4): 1347–1367. https://doi.org/10.1193/040916eqs057m.

Campbell, K. W., and Y. Bozorgnia. 2008. "NGA ground motion model for the geometric mean horizontal component of PGA, PGV, PGD and 5% damped linear elastic response spectra for periods ranging from 0.01 to 10 s." *Earthquake Spectra* 24 (1): 139–171. https://doi.org/10.1193/1.2857546.

Chen, Q.-F., Y. Chen, and L. Chen. 1997. "Earthquake loss estimation with GDP and population data." *Acta Seimologica Sin.* 10 (6): 791–800. https://doi.org/10.1007/s11589-997-0011-5.

Cimellaro, G. P., A. M. Reinhorn, and M. Bruneau. 2010. "Framework for analytical quantification of disaster resilience." *Eng. Struct.* 32 (11): 3639–3649. https://doi.org/10.1016/j.engstruct.2010.08.008.

Cimellaro, G. P., C. Renschler, F. Reinhorn, and L. Arendt. 2016. "PEOPLES: A framework for evaluating resilience." *J. Struct. Eng.* 142 (10): 04016063. https://doi.org/10.1061/(ASCE)ST.1943-541X.0001514.

Coupland, R. M. 1994. "Epidemiological approach to surgical management of the casualties of war." *Br. Med. J.* 308 (6945): 1693–1697. https://doi.org/10.1136/bmj.308.6945.1693.

Ellingwood, B. R., H. Cutler, P. Gardoni, W. G. Peacock, J. W. van de Lindt, and N. Wang. 2016. "The Centerville Virtual Community: A fully integrated decision model of interacting physical and social infrastructure systems." *Sustainable Resilient Infrastruct.* 1 (3–4): 95–107. https://doi.org/10.1080/23789689.2016.1255000.

Fawcett, W., and C. S. Oliveira. 2000. "Casualty treatment after earthquake disasters: Development of a regional simulation model." *Disasters* 24 (3): 271–287. https://doi.org/10.1111/1467-7717.00148.

FEMA. 2003. *Earthquake loss estimation methodology: Technical manual*. Washington, DC: National Institute of Building for the FEMA.

FEMA. 2012a. *Performance assessment calculation tool*. FEMA P58-3. Redwood City, CA: Applied Technology Council.

FEMA. 2012b. *Seismic performance assessment of buildings*. FEMA P58-1. Redwood City, CA: Applied Technology Council.

Hassan, E. M., and H. Mahmoud. 2018. "A framework for estimating immediate interdependent functionality reduction of a steel hospital following a seismic event." *Eng. Struct.* 168 (Aug): 669–683. https://doi.org/10.1016/j.engstruct.2018.05.009.

Hassan, E. M., and H. Mahmoud. 2019. "Full functionality and recovery assessment framework for a hospital subjected to a scenario earthquake event." *Eng. Struct.* 188 (Jun): 165–177. https://doi.org/10.1016/j.engstruct.2019.03.008.

Ibarra, L. F., and H. Krawinkler. 2005. *Global collapse of frame structures under seismic excitations*. Technical Rep. No. 152. Stanford, CA: John A. Blume Earthquake Engineering Research Center, Dept. of Civil Engineering, Stanford Univ.

Idriss, I. M., and H. B. Seed. 1968. "Seismic response of horizontal soil layers." *J. Soil Found. Div.* 94 (4): 1003–1031.

Jacques, C. C., M. Eeri, J. Mcintosh, S. Giovinazzi, T. D. Kirsch, M. Eeri, and M. Eeri. 2014. "Resilience of the Canterbury hospital system to the 2011 Christchurch earthquake." *Earthquake Spectra* 30 (1): 533–554. https://doi.org/10.1193/032013EQS074M.

Kammouh, O., G. Dervishaj, and G. P. Cimellaro. 2018. "Quantitative framework to assess resilience and risk at the country level." *ASCE-ASME J. Risk Uncertainty Eng. Syst., A: Civ. Eng.* 4 (1): 04017033. https://doi.org/10.1061/AJRUA6.0000940.

Kirsch, T. D., J. Mitrani-Reiser, R. Bissell, L. M. Sauer, M. Mahoney, W. T. Holmes, and F. De La Maza. 2010. "Impact on hospital functions following the 2010 Chilean earthquake." *Disaster Med. Pub. Health Preparedness* 4 (2): 122–128. https://doi.org/10.1001/dmphp.4.2.122.

Lignos, D. G., and H. Krawinkler. 2012. *Sidesway collapse of deteriorating structural systems under seismic excitations*. Technical Rep. No. 177. Stanford, CA: John A. Blume Earthquake Engineering Research Center, Dept. of Civil Engineering, Stanford Univ.

Lin, P., and N. Wang. 2017. "Stochastic post-disaster functionality recovery of community building portfolios I: Modeling." *Struct. Saf.* 69 (Nov): 96–105. https://doi.org/10.1016/j.strusafe.2017.05.002.

Lin, P., and N. Wang. 2019. "A probabilistic framework for post-disaster functionality recovery of community building portfolios." In *Proc., 13th Int. Conf. on Applications of Statistics and Probability in Civil Engineering, ICASP13*, 1–8. Seoul: Seoul National University Library.

Lin, S.-Y., W.-C. Chuang, L. Xu, S. El-Tawil, S. M. J. Spence, V. R. Kamat, C. C. Menassa, and J. McCormick. 2019. "A framework for modeling interdependent effects in natural disasters: Application to wind engineering." *J. Struct. Eng.* 145 (5): 04019025. https://doi.org/10.1061/(ASCE)ST.1943-541X.0002310.

Masoomi, H., J. W. van de Lindt, and L. Peek. 2018. "Quantifying socioeconomic impact of a tornado by estimating population outmigration as a resilience metric at the community level." *J. Struct. Eng.* 144 (5): 04018034. https://doi.org/10.1061/(ASCE)ST.1943-541X.0002019.

McKenna, F., G. L. Fenves, and M. H. Scott. 2000. *Open system for earthquake engineering simulation*. Berkeley, CA: Univ. of California.

Miles, S. B., and S. E. Chang. 2003. *Urban disaster recovery: A framework and simulation model*. MCEER-03-0005. Buffalo, NY: Multidisciplinary Center for Earthquake Engineering Research.

Miles, S. B., and S. E. Chang. 2006. "Modeling community recovery from earthquakes." *Earthquake Spectra* 22 (2): 439–458. https://doi.org/10.1193/1.2192847.

Miles, S. B., and S. E. Chang. 2011. "ResilUS: A community-based disaster resilience model." *Cartography Geogr. Inf. Sci.* 38 (1): 36–51. https://doi.org/10.1559/1523040638136.

Mitrani-Reiser, J., M. Mahoney, W. T. Holmes, J. C. De La Llera, R. Bissell, and T. Kirsch. 2012. "A functional loss assessment of a hospital system in the Bío-Bío Province." Supplement, *Earthquake Spectra* 28 (S1): 473–502. https://doi.org/10.1193/1.4000044.

NCSA (National Center for Supercomputing Applications). 2018. "ERGO-EQ platform for multi-hazard assessment, response, and planning." Accessed August 1, 2018. http://ergo.ncsa.illinois.edu/product/software/.

NIST. 2010. *Evaluation of the FEMA P695 methodology for quantification of building seismic performance factors*. NIST GCR 10-917-8. Gaithersburg, MD: NIST.

Nobuhara, R., Y. Sumiyoshi, and M. Miyano. 2000. "Study of casualties due to earthquake disasters and other accidents in Japan." In *Proc., 12th World Conf. on Earthquake Engineering*, 1–6. Kanpur, India: Indian Institute of Technology Kanpur.

Nos, W. V. 2011. *Post-earthquake injuries treated at a field hospital—Haiti, 2010*. Morbidity Mortality Weekly Rep. No. 59. Atlanta: Centers for Disease Control and Prevention.

PEER (Pacific Earthquake Engineering Research Center). 2018. "PEER ground motion database." Accessed August 1, 2018. https://ngawest2.berkeley.edu/.

Sediek, O. A., S. El-Tawil, and J. McCormick. 2019. "A scalable framework for assessing seismic resilience of communities." In *Proc., ASCE Structures Congress*. Reston, VA: ASCE.

Statistical Atlas. 2018. "Population of Shelby County, Tennessee." Accessed August 15, 2018. https://statisticalatlas.com/county/Tennessee/Shelby-County/Population.

Sutley, E. J., J. W. Van De Lindt, and L. Peek. 2017. "Community-level framework for seismic resilience. I: Coupling socioeconomic characteristics and engineering building systems." *Nat. Hazards Rev.* 18 (3): 04016014. https://doi.org/10.1061/(ASCE)NH.1527-6996.0000239.

USGS. 2018. "Memphis, Shelby County seismic hazard maps and data download." Accessed August 1, 2018. https://earthquake.usgs.gov/hazards/urban/memphis/grid_download.php.

Vona, M., M. Mastroberti, L. Mitidieri, and S. Tataranna. 2018. "New resilience model of communities based on numerical evaluation and observed post seismic reconstruction process." *Int. J. Disaster Risk Reduct.* 28 (Jun): 602–609. https://doi.org/10.1016/j.ijdrr.2018.01.010.